

# Solitonic in-gap modes in a superconductor-quantum antiferromagnet interface

J. L. Lado<sup>1</sup> and M. Sigrist<sup>2</sup>

<sup>1</sup>*Department of Applied Physics, Aalto University, Espoo, Finland*

<sup>2</sup>*Institute for Theoretical Physics, ETH Zurich, 8093 Zurich, Switzerland*

(Dated: July 5, 2022)

Bound states at interfaces between superconductors and other materials are a powerful tool to characterize the nature of the involved systems, and to engineer elusive quantum excitations. In-gap excitations of conventional s-wave superconductors occur, for instance, at magnetic impurities with net magnetic moment breaking time-reversal symmetry. Here we show that interfaces between a superconductor and a quantum antiferromagnet can host robust in-gap excitations, without breaking time-reversal symmetry. We illustrate this phenomenon in a one-dimensional model system with an interface between a conventional s-wave superconductor and a one-dimensional Mott insulator described by a standard Hubbard model. This genuine many-body problem is solved exactly by employing a combination of kernel polynomial and tensor network techniques. We unveil the nature of such zero modes by showing that they can be adiabatically connected to solitonic solutions between a superconductor and a classical antiferromagnet. Our results put forward a new class of in-gap excitations between superconductors and a disordered quantum spin phase can be relevant for a wider range of heterostructures.

Topological modes emerging in condensed matter systems are among the most intriguing features in physics. Well-known examples are the electronic solitons in polyacetylene[1] or the Jackiw-Rebbi modes first introduced in high-energy theory[2]. In recent years the family of topological phases with extraordinary modes has been extended enormously to a multitude of novel systems with gapped bulk excitation spectra [3–5]. In almost all cases, such topological modes emerge in systems that can be described within the spectra of non-interacting electrons, whose single-particle Hamiltonians incorporate a non-trivial topology. Despite the large body of knowledge on topologically non-trivial excitations of non-interacting particles accumulated in recent years, the theoretical analysis of the many-body counterpart remains a formidable challenge.

Among the different in-gap states found in materials, those of superconductors have attracted special attention, because they might provide valuable information about the nature of the superconducting phase, even if it is topologically trivial. On the one hand, a classical magnetic impurity (a static magnetic moment) gives rise to in-gap Yu-Shiba-Rusinov states in s-wave superconductor, probing the vulnerability to the superconducting phase against time-reversal symmetry violation (spin polarization)[6–13]. On the other hand, in-gap states created by non-magnetic impurities provide a strong signature for unconventional superconductivity [14–17]

Increasing complexity, for instance, through heterostructures connecting a superconductor to materials of various properties offers an attractive platform to create new emergent phases [18–20]. This is the basis for a plethora of proposals to engineer Majorana bound states [21], to explore unusual Andreev physics[22–24] and even to design higher-dimensional topological superconductors.[25, 26] So far studies in this

direction have focused mainly on single-particle physics, [3–5] e.g. system in which the excitation spectrum can be treated in a mean-field picture. Therefore, extending the scope to interface physics involving the strongly correlated electron regime with dominant quantum fluctuations represents a rich playground for new physics which is largely unexplored [27–31].

In this Letter we demonstrate how solitonic in-gap modes can emerge at interfaces between a conventional superconductor and a quantum antiferromagnet without long-range order, both topologically trivial on their own. In particular, we show that time-reversal symmetry needs not to be broken and that these modes can be adiabatically connected with solitonic zero modes of the antiferromagnetically ordered phase violating time-reversal symmetry. In this way, we extend the set of situations where the composition of different materials can generate a non-trivial phase at interfaces.

We model our system by the following Hamiltonian of a one-dimensional chain, that allows us incorporate an interface between a conventional superconductor and a quantum antiferromagnet in the simplest way:  $H = H_{kin} + H_U + H_{SC}$ , where  $H_{kin}$  is the kinetic energy term in a tight-binding form,

$$H_{kin} = t \sum_{n,s} [c_{n,s}^\dagger c_{n+1,s} + c_{n+1,s}^\dagger c_{n,s}] + \sum_{n,s} \mu(n) c_{n,s}^\dagger c_{n,s}, \quad (1)$$

$H_U$  is the Hubbard interaction term with a position dependent  $U$

$$H_U = \sum_{n,s} U(n) c_{n,\uparrow}^\dagger c_{n,\uparrow} c_{n,\downarrow}^\dagger c_{n,\downarrow}, \quad (2)$$

and  $H_{SC}$  introduces conventional superconductivity in the mean-field formulation

$$H_{SC} = \sum_n \Delta(n) [c_{n\uparrow} c_{n\downarrow} + c_{n\downarrow}^\dagger c_{n\uparrow}^\dagger]. \quad (3)$$

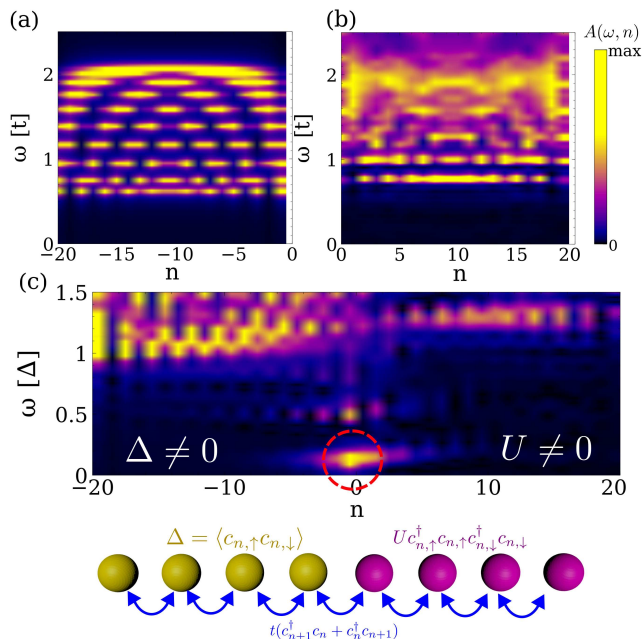


FIG. 1. (a) Spectral function of the superconductor, showing a gap up to the superconducting gap  $\Delta$ , and of the quantum antiferromagnet (b), showing a gap on the order of the Hubbard  $U$ . Panel (c) shows the spectral function across the interface between the two systems, showing the emergence of in-gap modes at the interface in the absence of time reversal symmetry breaking. We use  $\Delta = 0.6t$  and  $U = 4t$ . The inset below panel (c) shows a sketch of the model used to study the superconducting-antiferromagnetic interface.

The heterostructure can be modeled by the parametrization  $U(n) = [\tanh(n/W) + 1]U/2$ , and  $\Delta(n) = [\tanh(n/W) + 1]\Delta/2$  locating the interface at  $n = 0$  (Fig.1(a)), and we take  $W = 1$ . The profile of  $\mu(n)$  is chosen as  $\mu(n) = -U(n)/2$  so that the system is half filled everywhere. Our calculations are performed in chains having 40 sites.

For the treatment of this genuine many-body Hamiltonian we employ the computational matrix product formalism and, in particular, determine the local single-particle spectral function defined as

$$A(\omega, n) = \sum_s \langle GS | c_{n,s}^\dagger \delta(\omega - H + E_0) c_{n,s} | GS \rangle. \quad (4)$$

This dynamical correlation function can be computed for the whole frequency range by exploiting a kernel polynomial technique [32] implemented within the matrix product state formalism of ITensor [33, 34]. The basic idea of the method consists of representing the function  $A(n, \omega)$  in a complete functional basis expanded by  $N$  Chebyshev polynomials  $T_k(\omega)$  as  $A(n, \omega) = \frac{1}{\pi\sqrt{1-\omega^2}} \left( \mu_0 + 2 \sum_{k=1}^N \mu_k T_k(\omega) \right)$ . The coefficients  $\mu_k$  are obtained as  $\mu_k = \langle GS | c_n^\dagger T_k(H) c_n | GS \rangle$ , [35] that can be recursively computed through products of matrix product operators and matrix product states [32, 36–38].

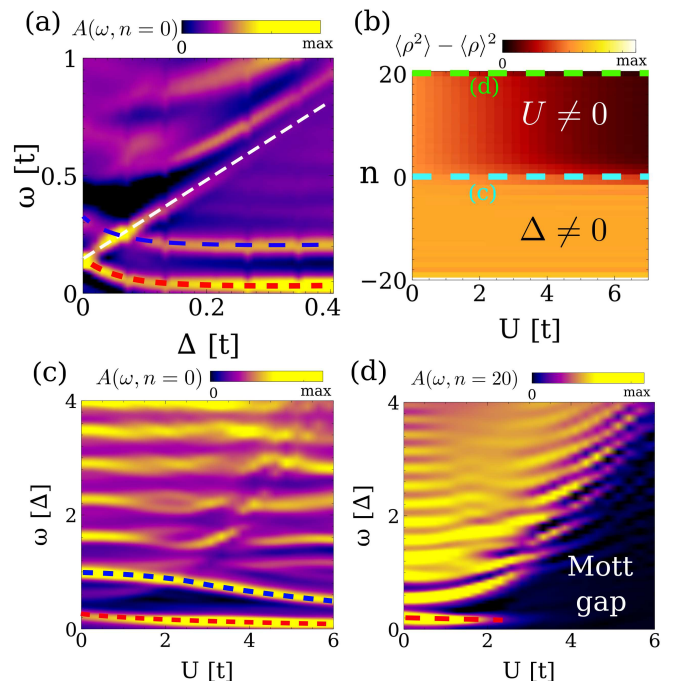


FIG. 2. (a) Evolution of the spectral function at the interface as a function of the superconducting pairing  $\Delta$ , for the other half chain with finite  $U$ . Panel (b,c,d) show the evolution as a function of  $U$  with the superconducting part at a fixed finite  $\Delta$ . Panel (b) shows the spatially resolved charge fluctuation in (b), the spectral function at the interface in (c) and the spectral function in the quantum antiferromagnetic part in (d). We use  $U = 6t$  for (a) and  $\Delta = 0.4t$  for (b,c,d).

Note that for this algorithm the time evolution is not needed, since we work from the beginning in frequency space.

The spectral function  $A(n, \omega)$  shows the quasiparticle excitation gap in real space. Thus, it is instructive to consider first each subsystem of the model separately using our computational scheme for a system of finite length. For the uniform superconductor,  $A(\omega, n)$  shows a quasiparticle gap (Fig.1(a)). The half-filled Hubbard chain with  $U > 0$  is not magnetically ordered, but displays a Mott charge excitation gap as seen in Fig.1(b)[39–41]. Note that the spatial dependence of the spectral functions in Fig.1(a,b) is a finite size effect induced by the open boundary conditions.

We turn now to the spatially resolved spectrum of a heterostructure connecting the two phases. As shown in Fig.1(c), the system shows now in-gap excitations (the lowest one highlighted with the dashed red circle), which are clearly a feature connected with the interface ( $n \approx 0$ ). Besides the previous in-gap mode, a second in-gap state at a higher energy can be observed at the interface in Fig.1(c). In-gap states in an s-wave superconductor are usually attributed to static magnetic impurities, giving rise to the so-called Yu-Shiba-Rusinov states. In our case,

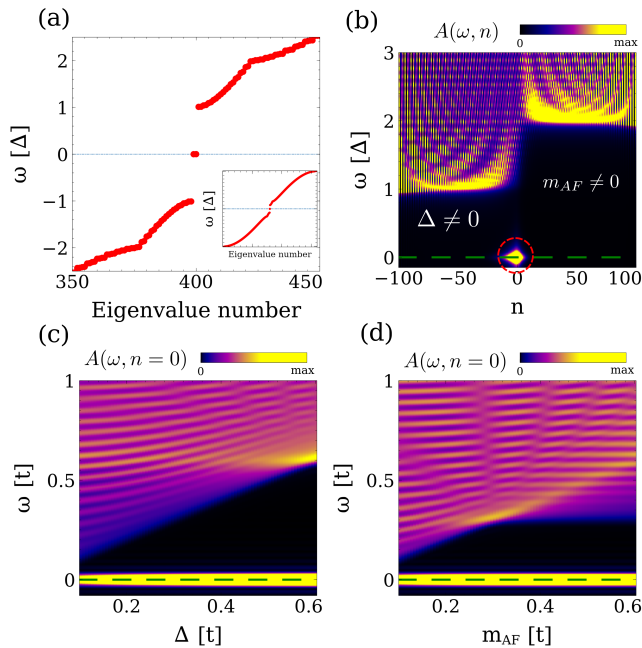


FIG. 3. (a) Bogoliubov de Gennes spectra of the superconductor-stagger antiferromagnet interface, showing the existence of a zero mode. Panel (b) shows the spatially resolved density of states of the interface, showing that the zero mode is localized at the interface between the two systems. Panel (c,d) show the evolution of the density of states at the interface as a function of the superconducting pairing  $\Delta$  (c) and the antiferromagnetic stagger field  $m_{AF}$  (d), highlighting the robustness of the zero mode. We use for (a,b)  $m_{AF} = 0.4t$  and  $\Delta = 0.2t$ , for (c)  $m_{AF} = 0.8t$  and for (d)  $\Delta = 0.3t$ . Note that the  $\omega$  axis starts slightly below  $\omega = 0$  for visibility, dark green dashed lines mark  $\omega = 0$  in (b,c,d).

however, time-reversal symmetry is conserved and there are no static moments despite the suppression of charge fluctuation on the Mott side ( $n > 0$ ). Moreover, the dominant mode here is essentially pinned at zero, a feature that does not happen for generic Yu-Shiba-Rusinov states.

Let us now consider the properties of this interface excitation. First, we examine how the interface mode behaves for varying the model parameters  $\Delta$  and  $U$ . In Fig.2(a) the spectral function  $A(\omega, n = 0)$  as function of  $\Delta$  for fixed  $U = 6t$  shows the evolution of the lowest mode toward  $\omega = 0$  upon increasing  $\Delta$ . With increasing  $\Delta$  the two in-gap modes (red and blue dashed line in Fig. 2(a)) converge to stable in-gap energies, while the bulk superconducting gap increases (white dashed line, note the shift due to finite size effects). Figs.2(b-d) display the  $U$ -dependence for fixed  $\Delta = 0.4t$ . In Fig. 2(b) we show how the charge fluctuations are gradually suppressed in the Mott region, while they remain constant in the superconducting region. The zero-energy mode (red dashed line) also settles at the interface upon increasing  $U$  as shown in Fig.2(c), and similar behavior

happens with the next in-gap state (blue dashed line). For comparison, we observe that the low-energy modes progressively fade away in the interior of the Mott region when  $U$  is increased (see Fig.2(d)).

A further path to elucidate the character of the zero-energy modes runs via the using a classical antiferromagnetic phase for  $n > 0$ . We restrict to the single-particle description by replacing  $H_U$  by  $H_{AF} = \sum_n (-1)^n m_{AF}(n) [c_{n\uparrow}^\dagger c_{n\uparrow} - c_{n\downarrow}^\dagger c_{n\downarrow}]$  with the spatial profile  $m_{AF}(n) = [1 + \tanh(n/W)]m_{AF}/2$  and  $\Delta(n) = [1 - \tanh(n/W)]\Delta/2$ . The Hamiltonian for this inhomogeneous 1D system can be easily solved numerically by means of a Bogoliubov de Gennes (BdG) scheme with the results displayed in Fig.3. We find zero-energy modes within the gap in the sequence of eigenvalues (Fig.3(a)) and can locate them clearly at the interface (Fig.3(b)). When changing the system parameters  $\Delta$  for fixed  $m_{AF} = 0.8t$  (Fig. 3(c)) and  $m_{AF}$  for fixed  $\Delta = 0.3t$  (Fig.3(d)) we observed that this mode remains solidly at  $\omega = 0$ , which demonstrates clearly that this feature is not an effect of fine-tuning.

The nature of this interface mode can be easily explained with an analytical approach in the continuum limit of this model. For this purpose we choose a two-site unit cell adapted to the staggered moment ( $A$  and  $B$  sublattice) and rewrite the kinetic energy term in  $k$ -space,

$$H(k) = \begin{pmatrix} 0 & 1 + e^{ik} \\ 1 + e^{-ik} & 0 \end{pmatrix} \quad (5)$$

which near  $k = \pi$  takes the form of a 1D Dirac equation with  $H(p) = \tau_y p$ , with  $\tau_y$  the sublattice Pauli matrix. We now use  $p = -i\partial_x$ , introduced into the adapted  $H_{AF}$  and  $H_{SC}$  and turn to continuum variables  $c_{2n} \rightarrow \psi_A(x)$ ,  $c_{2n+1} \rightarrow \psi_B(x)$ ,  $\Delta(n) \rightarrow \Delta(x)$ ,  $m_{AF}(n) \rightarrow m_{AF}(x)$  defining the continuum 1D Hamiltonian,

$$H = \sum_{s,\alpha,\beta} p \tau_y^{\alpha\beta} \psi_{\alpha,s}^\dagger \psi_{\beta,s} + \sum_{s,\alpha} m_{AF}(x) \sigma_z^{ss} \psi_{\alpha,s}^\dagger \psi_{\alpha,s} + \frac{1}{2} \sum_{\alpha} \Delta(x) [\psi_{\alpha,\uparrow} \psi_{\alpha,\downarrow} + \psi_{\alpha,\downarrow}^\dagger \psi_{\alpha,\uparrow}^\dagger] \quad (6)$$

This Hamiltonian can be diagonalized defining the Nambu spinor  $\Psi = (\psi_{A,\uparrow}, \psi_{B,\uparrow}, \psi_{A,\downarrow}^\dagger, \psi_{B,\downarrow}^\dagger)$ , for the sector of spin-up electron/spin-down hole, where we obtain  $H = \frac{1}{2} \Psi^\dagger \mathcal{H} \Psi$  with

$$\mathcal{H} = \begin{pmatrix} m_{AF}(x) & ip & \Delta(x) & 0 \\ -ip & -m_{AF}(x) & 0 & \Delta(x) \\ \Delta(x) & 0 & m_{AF}(x) & -ip \\ 0 & \Delta(x) & ip & -m_{AF}(x) \end{pmatrix}. \quad (7)$$

The spectrum is obtained by BdG transformation. While both the superconductor and the antiferromagnet have

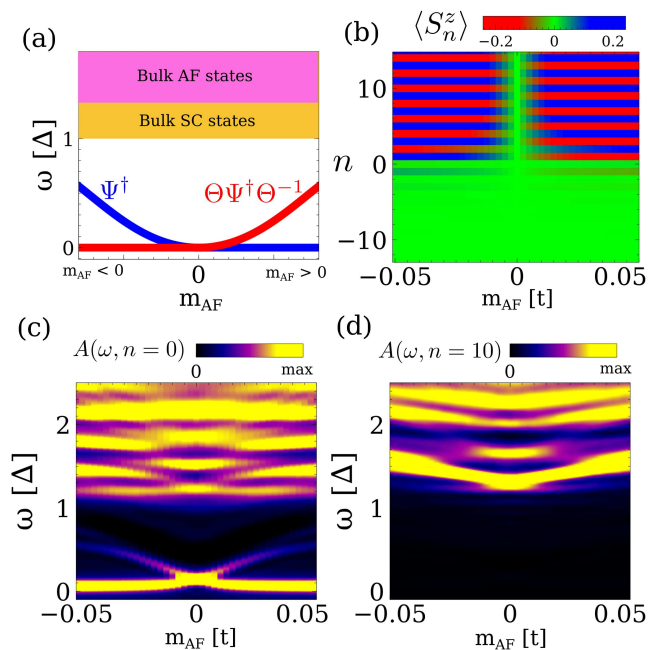


FIG. 4. (a) Sketch of the evolution of the charge excitation in the heterostructure, including the solitonic zero modes, as a function of the antiferromagnetic field  $m_{AF}$ , showing that they become the in-gap excitations in the case of the quantum antiferromagnet. (b) Spatially resolved magnetization as a function of  $m_{AF}$ . Panels (c,d) show the spectral function at the interface (c) and in the middle of the antiferromagnetic region (d). We use  $U = 6t$  and  $\Delta = 0.3t$ .

an excitation gap, we find at the interface a zero-energy eigenvalue with an eigenoperator [2, 42–44],

$$\Psi^\dagger = \frac{1}{2} [c_{A,\uparrow}^\dagger + c_{B,\uparrow}^\dagger - c_{A,\downarrow} + c_{B,\downarrow}] e^{\int_{-\infty}^x [m_{AF}(x') - \Delta(x')] dx'} \quad (8)$$

Note that since Eq. 7 is a real differential equation, the solitonic zero-mode Eq. 8 has real coefficients. It is also worth to note that time-reversal symmetry  $\Theta$  is not a symmetry of the interface. As a result, for the time-reversal counterpart of the previous system, the zero-mode excitation will be  $\Theta\Psi^\dagger\Theta^{-1}$ , different from  $\Psi^\dagger$ . Intuitively, the action of time reversal symmetry is equivalent to switching between positive or negative magnetic moments. In the non-interacting Hamiltonian presented, the zero-energy mode can be derived analytically, yet an analogous approach is not available if we replace the classical by a quantum antiferromagnet where the many-body nature of the system is important.

Although the many-body problem is challenging, we may connect with the previous solitonic mode by extending the many-body Hamiltonian with a staggered field on the Mott side, i.e.  $H = H_{kin} + H_U + H_{SC} + H_{AF}$ . In this way, we introduce a static moment in addition to the quantum fluctuation. This model shall again be solved by our computational many-body scheme. The

schematic result obtained is shown in Fig. 4(a), that shows that the two time-reversal related solutions found in the single-particle case, merge in the pure quantum limit yielding localized in-gap mode. The previous sketch captures only the single-particle charge excitations reflected in the correlator Eq. 4, whereas the many-body spectrum will show a continuum of states stemming from the gapless spinon modes of the quantum antiferromagnet. The transition from the quantum to the classical regime as the stagger magnetization is switched on can be directly observed in the expectation value of the local magnetic moment, as shown in Fig. 4(b).

We now verify the previous picture by examining the spectral function Eq. 4 at the interface,  $n = 0$  (Fig.4(c)) and at  $n = 10$  inside the Mott region (Fig.4(d)). We can observe how the in-gap mode is present for  $m_{AF} = 0$  and gradually transforms into the zero-energy solitonic mode just described, while the spectrum within the Mott region remains gapped. Thus, the in-gap spectrum of the many-body system is adiabatically connected to time-reversal symmetry breaking situation where low-energy quantum fluctuations are progressively suppressed upon increasing  $|m_{AF}|$ .

An interesting feature is the splitting of in-gap mode into two branches when  $m_{AF}$  is switched on, whereby only one branch evolves into the solitonic zero-energy mode, while second rises in energy and gradually loses weight. Moreover, it is also important to note that depending on the sign of  $m_{AF}$ , the low-energy mode will transform either into  $\Psi^\dagger$  or into  $\Theta\Psi^\dagger\Theta^{-1}$ . In the quantum antiferromagnetic regime, the two modes coexist, such that there is a two-fold degeneracy for the in-gap mode at  $m_{AF} = 0$ , whose energy needs not to lie at exactly zero.

To summarize, we have put forward a minimal system consisting of a many-body quantum antiferromagnet and a conventional s-wave superconductor that host solitonic in-gap excitations. We have unveiled the nature of those states, by showing that they can be adiabatically connected to solitonic states between a classical antiferromagnet and a superconductor, which resembles the Jackiw-Rebbi soliton. Our results put forward a minimal example in which solitonic modes appear between a quantum disordered magnet and a superconductor, providing a stepping stone towards the study of interfaces between superconductors and quantum spin liquids.

**Acknowledgments** M.S. is grateful for the financial support from the Swiss National Science Foundation (SNSF) through Division II (No. 163186 and 184739). J.L.L. acknowledges the computational resources provided by the Aalto Science-IT project.

- 
- [1] W. P. Su, J. R. Schrieffer, and A. J. Heeger, *Phys. Rev. Lett.* **42**, 1698 (1979).
- [2] R. Jackiw and C. Rebbi, *Phys. Rev. D* **13**, 3398 (1976).
- [3] X.-L. Qi and S.-C. Zhang, *Rev. Mod. Phys.* **83**, 1057 (2011).
- [4] M. Z. Hasan and C. L. Kane, *Rev. Mod. Phys.* **82**, 3045 (2010).
- [5] Y. Ando and L. Fu, *Annual Review of Condensed Matter Physics* **6**, 361 (2015).
- [6] J. O. Island, R. Gaudenzi, J. de Bruijkere, E. Burzurí, C. Franco, M. Mas-Torrent, C. Rovira, J. Veciana, T. M. Klapwijk, R. Aguado, and H. S. J. van der Zant, *Phys. Rev. Lett.* **118**, 117001 (2017).
- [7] D.-J. Choi, C. G. Fernández, E. Herrera, C. Rubio-Verdú, M. M. Ugeda, I. Guillamón, H. Suderow, J. I. Pascual, and N. Lorente, *Phys. Rev. Lett.* **120**, 167001 (2018).
- [8] M. Ruby, F. Pientka, Y. Peng, F. von Oppen, B. W. Heinrich, and K. J. Franke, *Phys. Rev. Lett.* **115**, 087001 (2015).
- [9] W. Chang, V. E. Manucharyan, T. S. Jespersen, J. Nygård, and C. M. Marcus, *Phys. Rev. Lett.* **110**, 217005 (2013).
- [10] M. Ruby, Y. Peng, F. von Oppen, B. W. Heinrich, and K. J. Franke, *Phys. Rev. Lett.* **117**, 186801 (2016).
- [11] M. Ruby, B. W. Heinrich, Y. Peng, F. von Oppen, and K. J. Franke, *Phys. Rev. Lett.* **120**, 156803 (2018).
- [12] B. M. Andersen, K. Flensberg, V. Koerting, and J. Paaske, *Phys. Rev. Lett.* **107**, 256802 (2011).
- [13] L. Cornils, A. Kamlapure, L. Zhou, S. Pradhan, A. A. Khajetoorians, J. Fransson, J. Wiebe, and R. Wiesendanger, *Phys. Rev. Lett.* **119**, 197002 (2017).
- [14] A. I. Larkin, *Soviet Journal of Experimental and Theoretical Physics Letters* **2**, 130 (1965).
- [15] A. J. Millis, S. Sachdev, and C. M. Varma, *Phys. Rev. B* **37**, 4975 (1988).
- [16] R. J. Radtke, K. Levin, H.-B. Schüttler, and M. R. Norman, *Phys. Rev. B* **48**, 653 (1993).
- [17] A. P. Mackenzie, R. K. W. Haselwimmer, A. W. Tyler, G. G. Lonzarich, Y. Mori, S. Nishizaki, and Y. Maeno, *Phys. Rev. Lett.* **80**, 161 (1998).
- [18] R. M. Lutchyn, J. D. Sau, and S. Das Sarma, *Phys. Rev. Lett.* **105**, 077001 (2010).
- [19] S. Nadj-Perge, I. K. Drozdov, J. Li, H. Chen, S. Jeon, J. Seo, A. H. MacDonald, B. A. Bernevig, and A. Yazdani, *Science* **346**, 602 (2014).
- [20] L. Fu and C. L. Kane, *Phys. Rev. Lett.* **100**, 096407 (2008).
- [21] J. Alicea, *Reports on Progress in Physics* **75**, 076501 (2012).
- [22] Y. Tanaka, Y. Mizuno, T. Yokoyama, K. Yada, and M. Sato, *Phys. Rev. Lett.* **105**, 097002 (2010).
- [23] F. Hübner, M. J. Wolf, T. Scherer, D. Wang, D. Beckmann, and H. v. Löhneysen, *Phys. Rev. Lett.* **109**, 087004 (2012).
- [24] X.-J. Liu, *Phys. Rev. Lett.* **109**, 106404 (2012).
- [25] F. Schindler, A. M. Cook, M. G. Vergniory, Z. Wang, S. S. P. Parkin, B. A. Bernevig, and T. Neupert, *Science Advances* **4**, eaat0346 (2018).
- [26] Z. Yan, *Phys. Rev. B* **100**, 205406 (2019).
- [27] K. A. Al-Hassanieh, J. Rincón, G. Alvarez, and E. Dagotto, *Phys. Rev. Lett.* **114**, 066401 (2015).
- [28] R. Thomale, S. Rachel, and P. Schmitteckert, *Phys. Rev. B* **88**, 161103 (2013).
- [29] D. Sticlet, L. Seabra, F. Pollmann, and J. Cayssol, *Phys. Rev. B* **89**, 115430 (2014).
- [30] A. E. Feiguin, S. R. White, and D. J. Scalapino, *Phys. Rev. B* **75**, 024505 (2007).
- [31] A. Haim, A. Keselman, E. Berg, and Y. Oreg, *Phys. Rev. B* **89**, 220504 (2014).
- [32] A. Weiße, G. Wellein, A. Alvermann, and H. Fehske, *Rev. Mod. Phys.* **78**, 275 (2006).
- [33] ITensor Library (version 2.0.11) <http://itensor.org>.
- [34] <https://github.com/joselado/dmrgpy>.
- [35] The Hamiltonian must be scaled to the interval (-1,1) to perform the Chebyshev expansion.
- [36] F. A. Wolf, I. P. McCulloch, O. Parcollet, and U. Schollwöck, *Phys. Rev. B* **90**, 115124 (2014).
- [37] F. A. Wolf, J. A. Justiniano, I. P. McCulloch, and U. Schollwöck, *Phys. Rev. B* **91**, 115144 (2015).
- [38] J. L. Lado and O. Zilberberg, *Phys. Rev. Research* **1**, 033009 (2019).
- [39] K. Penc, K. Hallberg, F. Mila, and H. Shiba, *Phys. Rev. Lett.* **77**, 1390 (1996).
- [40] Z. Chen, X. Li, and T. K. Ng, *Phys. Rev. Lett.* **120**, 046401 (2018).
- [41] M. Gulácsi and K. S. Bedell, *Phys. Rev. Lett.* **72**, 2765 (1994).
- [42] P. San-Jose, J. L. Lado, R. Aguado, F. Guinea, and J. Fernández-Rossier, *Phys. Rev. X* **5**, 041042 (2015).
- [43] J. L. Lado and M. Sigrist, *Phys. Rev. Lett.* **121**, 037002 (2018).
- [44] A. L. R. Manesco, G. Weber, and D. Rodrigues, *Phys. Rev. B* **100**, 125411 (2019).